Bioresource Technology 342 (2021) 125932

Contents lists available at ScienceDirect

Bioresource Technology

journal homepage: www.elsevier.com/locate/biortech

Comparison of different chemical treatments of brush and flat carbon electrodes to improve performance of microbial fuel cells

Emmanuel U. Fonseca [a], Wulin Yang [a,b], Xu Wang [c], Ruggero Rossi [a], Bruce E. Logan [a,*]

[a] Department of Civil and Environmental Engineering, The Pennsylvania State University, 231Q Sackett Building, University Park, PA 16802, United States
[b] College of Environmental Sciences and Engineering, Peking University, Beijing 100871, China
[c] School of Resource and Environmental Sciences, Wuhan University, Wuhan 430079, China

HIGHLIGHTS

- Anodes in MFCs were treated with TiO_2 or CNT particles, or an ionic liquid.
- Brush anode performance was not improved compared to a heat treated control.
- Flat anodes had lower power densities and higher resistances than brush anodes.
- CNT treatment of a carbon cloth flat anode improved power by 3.2 times.
- Other MFC resistances may limit improvements possible with brush anodes.

GRAPHICAL ABSTRACT

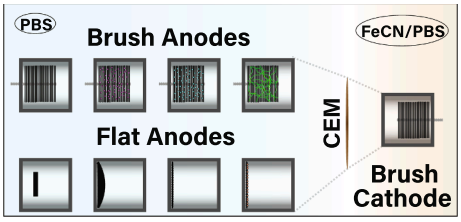

ARTICLE INFO

Keywords:
Brush anode
Ferricyanide cathode
Nanoparticles
Ionic liquid polymer
Carbon nanotubes

ABSTRACT

Anodes in microbial fuel cells (MFCs) can be chemically treated to improve performance but the impact of treatment on power generation has not been examined for different electrode base materials. Brush or flat anodes were chemically treated and then compared in identical two-chambered MFCs using the electrode potential slope (EPS) analysis to quantify the anode resistances. Flat carbon cloth anodes modified with carbon nanotubes (CNTs) produced 1.42 ± 0.06 W m^{-2}, which was 3.2 times more power than the base material (0.44 ± 0.00 W m^{-2}), but less than the 2.35 ± 0.1 W m^{-2} produced using plain graphite fiber brush anodes. An EPS analysis showed that there was a 90% decrease in the anode resistances of the CNT-treated carbon cloth and a 5% decrease of WO_3 nanoparticle-treated brushes compared to unmodified controls. Certain chemical treatments can therefore improve performance of flat anodes, but plain brush anodes achieved the highest power densities.

1. Introduction

Microbial fuel cells (MFCs) can be used to produce electricity by coupling the oxidation of organic matter by bacteria on the anode with the oxygen reduction reaction (ORR) at the cathode (Li et al., 2014a, Li et al., 2014b; Logan et al., 2015, 2006; Wan et al., 2016). Many types of anode materials have been used in MFCs, including graphite fiber brushes, carbon cloth, and carbon felt, and chemical treatments of these materials have been used to try to improve performance (Ahn and Logan, 2013; Cheng and Logan, 2007; Guo et al., 2013; Li et al., 2014a, Li et al., 2014b; Logan et al., 2007; Saito et al., 2011; Santoro et al., 2017; Wang et al., 2009). Although some electrode modifications have been demonstrated to improve performance based on power production for a single chemical treatment on one type of base material such as

* Corresponding author.
E-mail address: blogan@psu.edu (B.E. Logan).

https://doi.org/10.1016/j.biortech.2021.125932
Received 5 August 2021; Received in revised form 6 September 2021; Accepted 8 September 2021
Available online 13 September 2021

carbon cloth, there have been no comparisons of the effect of treatments using different base materials (Ge et al., 2016; Lanas et al., 2014; Yang and Logan, 2016; Zhang et al., 2014). It is also not possible to compare the impact of these treatments based on reported power densities between different studies as the amount of baseline power produced (no treatment) is a function of any differences in MFC conditions, such as electrode projected areas (Cheng et al., 2014; Dewan et al., 2008; Rossi et al., 2019c), electrode spacing (Logan et al., 2018; Rossi et al., 2019b), and electrode sizes relative to each other (for example a cathode larger than the anode) (Fan et al., 2008; Lanas and Logan, 2013). A change in percentage of maximum power density achieved with one type of anode base material therefore cannot be used to predict performance in another type of MFC with different configurations (Logan, 2010). Even with identical reactors power can vary between different laboratories (Yang et al., 2017), and therefore it is important to examine different chemical treatments of anodes under otherwise identical conditions.

The impact of an anode material or chemical treatment of an anode can be more directly quantified by examining electrode resistances, using the electrode potential slope (EPS) analysis, than just noting the maximum power density which is also a function of the cathode and ohmic resistances. The EPS method can be used to calculate the anode resistance, relative to the solution and cathode resistances, using electrode polarization data in order to quantify the anode resistance relative to the total internal resistance (Cario et al., 2019; Lawson et al., 2020; Rossi et al., 2020, 2019a; Rossi and Logan, 2020). MFCs contain three different regions in polarization curves: an activation loss dominated region characteristic of a sharp potential drop at low current densities, a linear region dictated by ohmic resistances, and a rapid decrease to voltage at high current densities due to mass transfer limitations (Feng et al., 2010a, Feng et al., 2010b; Nguyen et al., 2016; Rismani-Yazdi et al., 2008; Wen et al., 2009). Using the linear region near peak power production with the EPS method, and normalizing by the electrode area, enables calculation of the area-based resistance (mΩ m^2) from the slope of the polarization data. For example, an EPS analysis has shown that increasing phosphate buffer concentrations (from 50 mM to 200 mM) improved power due to a 64% decrease in the anode resistance (Rossi et al., 2020). A microbial electrolysis cell (MEC) application of the EPS method showed that the anode resistance (71 ± 5 mΩ m^2) contributed a total of 59% of the total internal resistance (120 ± 0 mΩ m^2), and therefore it was the main factor limiting MEC performance (Cario et al., 2019). Therefore, it is possible to improve MFC or MEC performance by reducing the anode resistance when it is a predominant resistance in the system (Fan et al., 2008; Liang et al., 2007; Sleutels et al., 2009).

Chemical modifications of the anode have been used to improve performance in terms of power production (Cheng and Logan, 2007; Guo et al., 2013; Li et al., 2014a, Li et al., 2014b; Saito et al., 2011; Wang et al., 2009), but the relative contribution of anode material to the overall internal resistance also needs to be examined to determine the possible amount of impact from the specific chemical treatment. For example, a large change in power could be produced by anode treatment in a system where the anode resistance was a high proportion of the total internal resistance, but only a small change in power would be observed in another MFC if the anode resistance was only a small part of the total internal resistance.

The objective of this study was to examine if chemical treatments applied to flat and brush anodes could be used to improve power production. To examine the impact of chemical modifications of anodes on the performance of MFCs, power production was examined using two-chambered MFCs. Chemical treatments were selected from those shown in previous studies to facilitate bioelectrochemical interactions of bacteria with the anode or improve power. These treatments included addition of electrically conductive particles where surface charge and electrical conductivity were improved by using carbon nanotubes (CNTs) (Ronen et al., 2015) or with semiconductor nanoparticles (e.g. TiO_2 and WO_3) (Yang et al., 2016; Zhang et al., 2015, 2017; Zhou et al., 2018), and the application of a positively charged ionic liquid polymer that was shown to improve current densities by an order of magnitude (Saito et al., 2010; Wang et al., 2016, Wang et al., 2011). Brush anodes, which have been shown to produce high power densities in MFCs, were examined here as the base material with three of these different chemical treatments. In addition, three different flat anode materials (graphite, carbon cloth and carbon felt) were used as controls to demonstrate the impact of the base electrode materials on anode resistance relative to the total internal resistance. One of the flat materials (carbon cloth) was also examined using the carbon nanotube treatment to show the impact of this chemical treatment on a flat anode relative to the brush anode. A ferricyanide ($Fe(CN)_6^{3-}$) catholyte was used to provide consistent cathode performance and to improve power production due to an ~ 270 mV increase to the cathode working potentials relative to those obtained using air cathodes (Lawson et al., 2020). The impacts of these chemical treatments were evaluated based on changes in the three component resistances (anode, cathode, and solution) and the working half-cell potentials using the EPS method (Cario et al., 2019; Lawson et al., 2020; Rossi et al., 2020, 2019a; Rossi and Logan, 2020).

2. Materials and methods

2.1. Electrode fabrication

A total of eight anodes were tested with brush anodes treated in three different ways and a plain brush as a control, and four planar (flat) anodes (Fig. 1). All electrode materials, including the brush cathodes, were heat treated at 450 °C for 30 min in a muffle furnace prior to use or modification to remove manufacturing impurities (Feng et al., 2010a, Feng et al., 2010b). The graphite fiber brushes were made using two twisted titanium wires (Zoltec PX35 graphite fibers; Mill-Rose, OH, USA) with fiber occupying a length of 2.5 cm and diameter of 2.5 cm (Logan et al., 2007). The four brush anodes were: a brush modified with TiO_2 nanoparticles (B_{TIO2}), a brush modified with WO_3 nanoparticles (B_{WO3}), a brush modified with an ionic conductive polymer (B_{ICP}), and an unmodified brush (B) as a control. The nanoparticle modified brushes were made from brushes dip-coated in nanoparticle solutions, 100 μM TiO_2 (<25 nm particle size; Sigma-Aldrich, MO, USA) for the B_{TIO2} electrodes and 100 μM WO_3 (<100 nm particle size; Sigma-Aldrich, MO, USA) for the B_{WO3} electrodes. The B_{ICP} electrodes were brushes modified by dip-coating in an anion exchange polymer solution made from a mixture of quaternary DABCO (1,4-diazabicyclo [2.2.2] octane) polysulfone (QDPSU) and carbon black (Wang et al., 2011). Carbon black (Vulcan XC-72R; Cabot, MA, USA) and QDPSU, prepared as previously reported (Wang et al., 2016), were weighted at a ratio of 1:1 and then dispersed in dimethylacetamide (5% wt). After these modifications, brushes all were dried in a vacuum desiccator for 30 min at 70 °C and finally stored at room temperature.

The flat anodes tested were three unmodified materials, a graphite block (F_G), carbon felt (F_{CF}), carbon cloth (F_{CC}), and carbon cloth modified with carbon nanotubes ($F_{CC/CNT}$). The F_G electrodes (Morgan Advanced Materials, Windsor, UK) were 5 mm thick squares with 2 cm long edges (4 cm^2). The F_{CF} (Alfa Aesar, MA, USA) and F_{CC} (BASF Fuel Cell Inc., NJ, USA) electrodes were cut into circular shapes with a diameter of 3 cm (~7 cm^2). The $F_{CC/CNT}$ (~7 cm^2) electrodes were fabricated by modifying the same carbon cloth material used in the F_{CC} reactors. Briefly, the CNT film was deposited on the carbon cloth by spray coating CNT and polyvinyl alcohol (PVA) layers (1 wt% PVA in DI water). The CNTs consisted of multi-walled carbon nanotubes, functionalized with carboxylic groups (CNTs–COOH), with 30–50 nm outer diameters and 10–20 nm lengths at a purity of > 95% (CheapTubes Inc., Brattleboro, VT, USA). The CNT coated carbon cloth was then submerged in a cross-linking solution, consisting of glutaraldehyde (50% wt) and diluted hydrochloric acid (37% wt), and heated at 90 °C for 1 h. Afterwards, the CNT coated carbon cloth was oven dried at 90 °C for 5 min and stored at room temperature (Ronen et al., 2015).

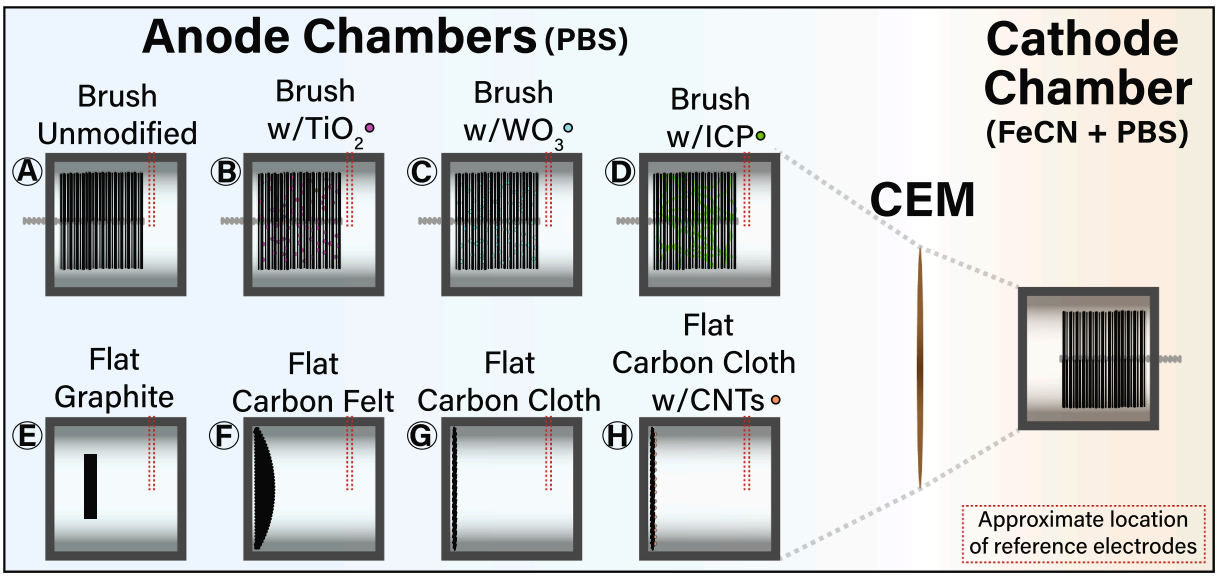

Fig. 1. Configuration of the two-chambered MFCs. The four brush anode materials tested are shown in the top row and include an unmodified brush (A, B), a brush modified with TiO_2 nanoparticles (B, B_{TIO2}), a brush modified with WO_3 nanoparticles (C, B_{WO3}), and a brush modified with an ionic liquid polymer (D, B_{ICP}). The four planar, "flat" anode materials tested are shown in the bottom row and include an unmodified block of graphite (E, F_G), an unmodified carbon felt (F, F_{CF}), an unmodified carbon cloth (G, F_{CC}), and a carbon cloth modified with carbon nanotubes (H, $F_{CC/CNT}$).

Carbon brushes had 4300 m^2 per m^3 of reactor based on bristle area (Lanas and Logan, 2013) and carbon cloth had 2670 m^2 m^{-3} calculated using a technical data sheet indicating 50% porosity and fiber diameter of 7.5 μm (Fuel Cell Earth, 2021). The graphite blocks were assumed to be essentially flat with an exposed area of 360 m^2 m^{-3}. While these are large differences in intrinsic surface area, previous research has shown that the projected area of the electrode is more critical to power production than internal surface area (Lanas and Logan, 2013; Rossi and Logan, 2020). The anodes had 4.9 cm^2 (brush), 7.0 cm^2 (carbon cloth), and 4 cm^2 (graphite) of projected surface area per 7 cm^2 of cathode projected area.

2.2. MFC configuration and operation

A total of sixteen two-chambered MFCs were used, duplicate reactors for each of the eight anodes tested. Two-chambered MFCs were constructed from two blocks of polycarbonate drilled to have 28 mL chambers (3 cm diameter, 4 cm length), with the chambers separated by a cation exchange membrane (CEM; Selemion, Bellex International Corporation, DE, USA) (Fig. 1) (Lawson et al., 2020). The cathodes for all reactors were an unmodified brush fixed at 1 cm from the CEM. The brush anode (Fig. 1**A–D**) tips were arranged to be 1 cm from the CEM and in close contact (~1 mm) with the tip of the reference electrode (RE; Ag/AgCl, model RE-5B, BASi, IN, USA; +0.199 V versus a standard hydrogen electrode, SHE). The F_G anodes (Fig. 1**E**) were fastened to a titanium current collector and suspended by it in the center of the anode chamber fixed at 3 cm from the CEM and 2 cm from the RE. The F_{CF} anodes (Fig. 1**F**) were in contact with a titanium current collector and had an effective distance of 3.1 cm from the CEM and 2.1 from the RE (Logan et al., 2018). The F_{CC} and $F_{CC/CNT}$ anodes (Fig. 1**G–H**) were also in contact with a titanium current collector and were set at 4 cm from the CEM and 3 cm from the RE.

All reactors were operated in fed-batch mode with the solutions replenished every 1–2 days. The anolyte contained sodium acetate (2 g L^{-1}; equivalent to 1.5 g L^{-1} of COD) dissolved in a 50 mM phosphate buffer solution (PBS; 4.58 g Na_2HPO_4, 2.45 g NaH_2PO_4, 0.13 g KCl, and 0.31 g NH_4Cl in 1 L of deionized water) with added mineral and vitamin solutions (Rossi et al., 2020). The catholyte was 50 mM potassium ferricyanide ($K_3Fe[CN]_6$) dissolved in 50 mM PBS (Lawson et al., 2020; Rezaei et al., 2009).

Current generation was monitored every 20 min by measuring the voltage across a resistor, set to 1000 Ω during normal operation, with a multimeter (Model 2700, Keithley Instruments, Inc., OH). Anodes were inoculated with effluent from a well acclimated microbial fuel cell (50% anolyte buffer solution, 50% MFC effluent) for 7 days. After the inoculation period, only the anolyte buffer solution was fed into the anode chamber. All MFCs were acclimated for 6–8 weeks before further experimentation and were normally operated during this period in a constant temperature room set at 30 °C. Reproducible, stable voltage profiles were obtained for all reactors within the first 4 weeks of normal operation (Rossi et al., 2017).

2.3. Electrochemical characterization

Prior to polarization tests, MFCs were acclimated for two days at lower set resistances (100–500 Ω) to minimize the potential for power overshoot (a doubling back of the power curve) (Hong et al., 2011; Watson and Logan, 2011; Zhu et al., 2013). Single-cycle polarization tests were conducted by feeding the reactor with fresh medium, maintaining the system under open circuit conditions for 2 h, and then running linear sweep voltammetry (LSV) with a potentiostat (VMP3 Multichannel Workstation; Biologic Science Instruments, USA) (Rossi et al., 2020). LSV tests were performed in a three-electrode configuration, with the anode set as the working electrode, at a scan rate of 0.1 mV s^{-1} in a constant temperature room set at 30 °C. Electrochemical data was normalized by the CEM surface area (7 cm^2). Analysis of polarization test variability was performed by a two-sided *t*-test.

The EPS method was used to analyze LSV polarization data in terms of the whole cell and electrodes, corrected for solution resistance losses between the working electrodes and reference electrodes (Cario et al., 2019; Lawson et al., 2020; Rossi et al., 2020, 2019a; Rossi and Logan, 2020). The linear portion of the polarization data near the reactor's corresponding peak power production, where activation and diffusion losses are minimal, was analyzed with a least-squares regression and expressed as $E = mi + b$. The slope m is the specific resistance of each component (R_{int}, R_{cat}, R_{an}; mΩ m^2) and the y-intercepts are used to calculate experimental open circuit potentials ($E_{emf,e0}$, $E_{cat,e0}$, $E_{an,e0}$; V).

The solution resistance (R_Ω, mΩ m^2) was obtained from the solution

conductivity (σ, mS cm^{-1}; 1 S = 1 Ω^{-1}) and the distance between the electrodes (l, cm) as $R_\Omega = \frac{100l}{\sigma}$ where 100 is used for unit conversion (Rossi et al., 2019a). The solution conductivities were 8 mS cm^{-1} for the anolyte and 21 mS cm^{-1} for the catholyte. The membrane resistance (R_{mem}) was calculated as the difference between the sum of the individual resistances and the measured internal resistance of the reactor, $R_{mem} = R_{int} - (R_{an} + R_{cat} + R_\Omega)$ (Cario et al., 2019; Lawson et al., 2020), based on the whole cell polarization data of a four-electrode, one RE in each chamber, single-cycle LSV polarization test conducted on the B reactors. To minimize reactor performance impacts due to consecutive LSV tests, the four-electrode polarization test was performed after 2 weeks of normal operation following the three-electrode LSV polarization tests. Applying the EPS method to the four-electrode polarization data resulted in an $R_{mem} = 5.6 \pm 1.1$ mΩ m^2.

3. Results and discussion

3.1. MFC whole cell performance based on maximum power densities

The three chemically treated brushes all produced maximum power densities similar to the unmodified control based on polarization curves obtained using fully acclimated MFCs (Fig. 2). The maximum power density was 2.35 ± 0.09 W m^{-2} for the brush with no modification, which was comparable to that obtained using chemical treatments with WO_3 (B_{WO3}, 2.35 ± 0.01 W m^{-2}), TiO_2 (B_{TIO2}, 2.30 ± 0.08 W m^{-2}), and the ionic polymer (B_{ICP}, 2.26 ± 0.07 W m^{-2}). These maximum power densities were within 5% of those reported previously for two-chambered ferricyanide-catholyte MFCs of the same design, but they were > 70% higher than conventional air–cathode MFCs due to the additional voltage contributed by the ferricyanide reduction compared to oxygen reduction (Lawson et al., 2020; Rossi et al., 2019a; Yang et al., 2017).

The flat anode MFCs all produced lower maximum power densities than those produced using the chemically treated or unmodified brush electrodes (Fig. 2). The carbon felt anode MFCs produced the highest maximum power density of 1.46 ± 0.01 W m^{-2}, with a slightly lower power density with the graphite block of 1.35 ± 0.04 W m^{-2}, and a much lower power density with unmodified carbon cloth of 0.44 ± 0.00 W m^{-2}. Chemical treatment of the carbon cloth with carbon nanotubes tripled the maximum power production by the carbon cloth to 1.42 ± 0.06 W m^{-2}, demonstrating the effectiveness of treatment with electrically conductive particles for the flat anode but not for the graphite brush. However, the power produced by the carbon cloth following chemical treatment with carbon nanotubes was still similar to that of the other flat electrodes.

3.2. MFC electrode performance analyzed using the EPS method

To better understand the reasons for the differences in performance between the brushes and flat anodes, and the improved performance of the carbon cloth treated with CNTs but not the brush anode with conductive particles, polarization data were obtained for the electrodes. Cathode potentials were generally similar for all reactors although the current ranges for the cathode potentials were different (Fig. 3). The flat anode reactor cathodes operated only up to < 4.5 A m^{-2}. The brush anode MFC cathodes reached > 7 A m^{-2} but decreased by only ≤ 0.1 V over this larger range of current densities. The anode potentials appeared to be quite similar for all materials except for the unmodified carbon cloth electrodes when compared at the same current densities. The anode potentials at a given current density were also similar except the carbon cloth which increased to more positive potentials by + 0.1 V at current densities up to 4 A m^{-2} and by + 0.25 V or more for the brush anodes at current densities up to 8 A m^{-2}. This comparison of electrode potentials suggested that, except for the unmodified carbon cloth, there were relatively small differences between the potentials of the different anodes (Fig. 4) despite large differences in maximum power production

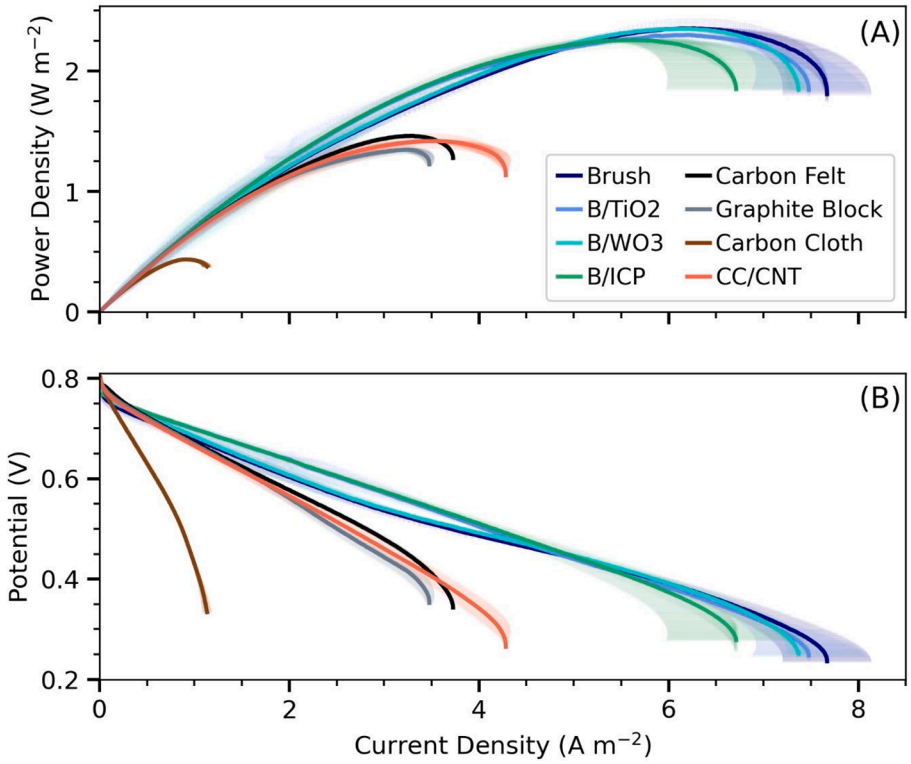

Fig. 2. Power density (A) and whole cell polarization (B) curves. The brush anode reactors are shown in blue hues and the four planar, "flat" anode reactors are shown in non-blue colors. Colored shadows represent standard deviations. (For interpretation of the references to colour in this figure legend, the reader is referred to the web version of this article.)

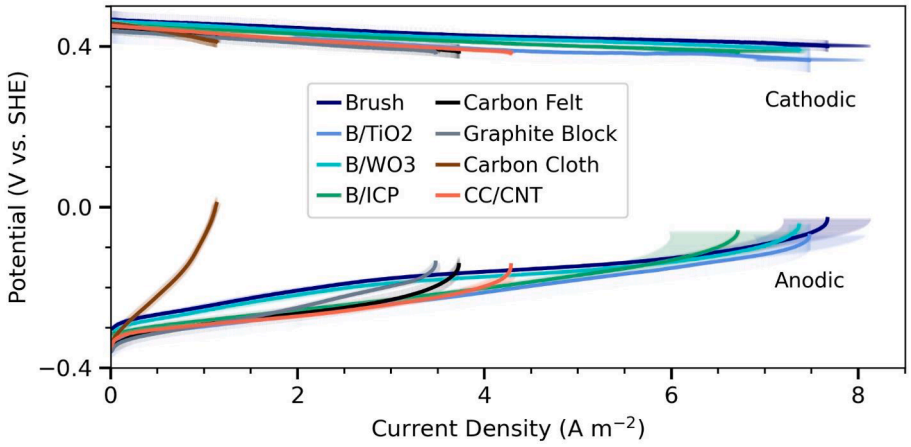

Fig. 3. Electrode polarization curves. Colored shadows represent the standard deviations.

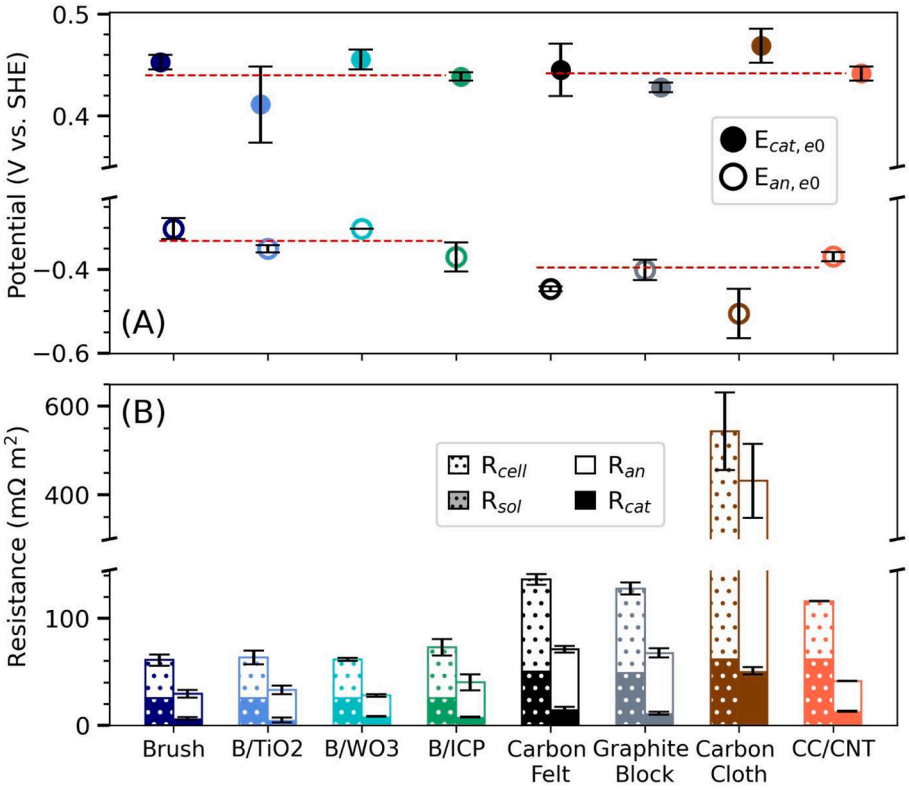

Fig. 4. Electrode potential slope analysis results, including experimental open circuit potentials (A) and internal resistances (B). The filled-in circles represent experimental open-circuit cathode potentials ($E_{cat,e0}$) and the hollow circles represent experimental open-circuit anode potentials ($E_{an,e0}$). The red, dashed lines represent the average experimental open-circuit potentials of the corresponding region. The dotted, filled-in bars represent solution resistances (R_{sol}) and the dotted, hollow bars represent whole cell resistances (R_{cell}). The undotted, filled-in bars represent cathode resistances (R_{cat}) and the undotted, hollow bars represent anode resistances (R_{an}). Error hatchbars represent the standard deviations.

shown between the brush and flat anodes, likely due to the different limiting current densities of the different anode materials (Fig. 2).

To further explore differences in performance the EPS method was used to determine the operating electrode potentials and resistances. The experimental cathode potentials near the point of maximum power production were the same when using different anode materials, with an average of $E_{cat,e0} = 440 \pm 26$ mV (vs. SHE) for the brush reactor cathodes and 442 ± 16 mV for the flat reactor cathodes (Fig. 4). However, the average anode potentials were more negative for the flat anodes ($E_{an,e0} = -395 \pm 42$ mV) compared to the brush anodes (-331 ± 37 mV). As current density increases the anode overpotentials will become more positive. Therefore, the flat anodes operating at lower current densities had slightly more negative potentials than those of the brush electrodes and, due to the lower average current densities, the flat anode reactors overall produced less power.

The reason for the higher power production by the brush anodes was their lower whole cell resistances, primarily due to lower solution resistances (Fig. 4). The brush anode MFCs had total internal resistances $<$ 75 mΩ m^2 while those of the flat anodes were $>$ 115 mΩ m^2. The large, highly porous brush anodes (2.5 cm long) spanned most of the anode chamber (4 cm long) with the end of the brush close to the CEM (~1 cm). Flat anodes were positioned here as is typical in air–cathode MFCs where they must be positioned 3–4 cm from the cathode to avoid excessive oxygen intrusion into the anode. Thus, the flat anode MFCs had a larger total solution resistance of $>$ 49 mΩ m^2 compared to $<$ 26 mΩ m^2 for the brush anodes. As a result of these different solution resistances, the power density comparison of brush and flat anode MFCs must be made based on anode performance, in terms of resistances, rather than on maximum power production.

When the brush and flat anodes were compared using the EPS analysis it was determined that the brush anode resistances were substantially lower than those of the flat anodes. The brush anodes ranged

from 28 ± 1 mΩ m^2 (B_{WO3}) to 40 ± 7 mΩ m^2 (B_{ICP}), compared to 68 ± 4 mΩ m^2 (F_G) to 432 ± 84 mΩ m^2 (F_{CC}) for the flat anodes (Fig. 4). Therefore, the use of the EPS method showed that the brushes did have improved performance based on their lower electrode resistances, although the higher maximum power densities of the brush reactors were also aided by having smaller solution resistances.

Chemical treatments did not appreciably impact the performance of the brush reactors, based on the resistances calculated using the EPS analysis, but did significantly improve the carbon cloth anode. While the resistance of the unmodified brush anode was 29 ± 4 mΩ m^2, the resistance of the brush anode modified with a conductive particle was similar at 28 ± 1 mΩ m^2 (B_{WO3}). Chemical treatment substantially improved the performance of the carbon cloth anode, which had the highest resistance of all the anode materials tests. The unmodified carbon cloth anode had a resistance of 432 ± 84 mΩ m^2, or 10.5 times that of the carbon cloth modified using CNTs (41 ± 0 mΩ m^2). Cathode resistance values were very low, averaging R_{cat} = 15 ± 14 mΩ m^2 (Fig. 4). These results for the different anodes demonstrated that chemical treatment could successfully improve performance if the original anode material performs poorly, but these treatments did not improve the performance of brush anodes which inherently have very low electrical resistances.

3.3. Implications for future MFC studies

Many chemical treatments have been used to improve MFC performance, but the treatments examined here have previously only been applied to flat anodes. As was shown here, when several of these chemical treatments were tested on brush anodes none of them increased the overall power production by the MFC. In addition, using the EPS analysis, it was shown that the treatment did not impact anode working potentials or the anode resistance of the brush anodes. Brush anodes are therefore already optimally suited for use in MFCs as they can be placed close to the cathode (~1 cm) without adverse impacts of oxygen intrusion through the cathode, compared to flat anodes which must be placed farther from the cathode to avoid adverse impacts of oxygen crossover through the cathode (Lawson et al., 2020; Rossi et al., 2020, 2019a; Rossi and Logan, 2020). Even after correcting for the higher solution resistances of the flat anodes, the brush anodes had improved performance compared to the chemically treated and unmodified flat anodes.

CNT treatment of a carbon cloth anode was used as a positive control. When this CNT-treated cloth anode was tested in the MFCs the power production increased 3.2-fold and the anode resistance was reduced by a factor of 10.5. Therefore, the CNT treatment could be effective but only in the case of the flat carbon anode that had the highest resistance of all the materials tested. This positive result with the flat anode showed that treatment with conductive particles had the potential to increase the brush anode performance, but since no improvement was observed, this suggests that the brush anode was already working well enough that other resistances in the system may have limited performance such as solution, membrane, or cathode resistances.

4. Conclusions

Chemical treatment of brush anodes using conductive particles or treatment with an ionic liquid polymer did not lower brush anode resistances or improve maximum power densities. MFCs with brush anodes had higher power compared to cells with flat anodes primarily due to the higher solution resistances in the flat anode reactors. However, based on the EPS analysis results that eliminated solution resistance as a performance factor, the brush anodes had lower resistances which demonstrate better performance overall compared to flat anodes. CNT treatment of carbon cloth anodes improved performance, but power was still less than that achieved with brush anodes.

CRediT authorship contribution statement

Emmanuel U. Fonseca: Conceptualization, Investigation, Validation, Writing - original draft. **Wulin Yang:** Methodology, Writing - review & editing, Supervision. **Xu Wang:** Methodology, Writing - review & editing. **Ruggero Rossi:** Writing - review & editing, Supervision. **Bruce E. Logan:** Conceptualization, Methodology, Writing - review & editing, Supervision, Funding acquisition.

Declaration of Competing Interest

The authors declare that they have no known competing financial interests or personal relationships that could have appeared to influence the work reported in this paper.

Acknowledgements

This work was conducted at the Pennsylvania State University and supported by funds provided by the US Department of Energy (DOE) Energy Efficiency and Renewable Energy (EERE) Fuel Cell Technologies Office, through a contract from the National Renewable Energy Laboratory (NREL), Project #21263, and Penn State University.

References

Ahn, Y., Logan, B.E., 2013. Altering anode thickness to improve power production in microbial fuel cells with different electrode distances. Energy and Fuels 27 (1), 271–276. https://doi.org/10.1021/ef3015553.

Cario, B.P., Rossi, R., Kim, K.-Y., Logan, B.E., 2019. Applying the electrode potential slope method as a tool to quantitatively evaluate the performance of individual microbial electrolysis cell components. Bioresour. Technol. 287, 121418. https://doi.org/10.1016/j.biortech.2019.121418.

Cheng, S., Logan, B.E., 2007. Ammonia treatment of carbon cloth anodes to enhance power generation of microbial fuel cells. Electrochem. Commun. 9 (3), 492–496. https://doi.org/10.1016/j.elecom.2006.10.023.

Cheng, S., Ye, Y., Ding, W., Pan, B., 2014. Enhancing power generation of scale-up microbial fuel cells by optimizing the leading-out terminal of anode. J. Power Sources 248, 931–938. https://doi.org/10.1016/j.jpowsour.2013.10.014.

Dewan, A., Beyenal, H., Lewandowski, Z., 2008. Scaling up microbial fuel cells. Environ. Sci. Technol. 42 (20), 7643–7648. https://doi.org/10.1021/es800775d.

Fan, Y., Sharbrough, E., Liu, H., 2008. Quantification of the internal resistance distribution of microbial fuel cells. Environ. Sci. Technol. 42 (21), 8101–8107. https://doi.org/10.1021/es801229j.

Feng, C., Li, F., Liu, H., Lang, X., Fan, S., 2010a. A dual-chamber microbial fuel cell with conductive film-modified anode and cathode and its application for the neutral electro-Fenton process. Electrochim. Acta 55 (6), 2048–2054. https://doi.org/10.1016/j.electacta.2009.11.033.

Feng, Y., Yang, Q., Wang, X., Logan, B.E., 2010b. Treatment of carbon fiber brush anodes for improving power generation in air-cathode microbial fuel cells. J. Power Sources. 195 (7), 1841–1844. https://doi.org/10.1016/j.jpowsour.2009.10.030.

Ge, B., Li, K., Fu, Z., Pu, L., Zhang, X., Liu, Z., Huang, K., 2016. The performance of nano urchin-like NiCo2O4 modified activated carbon as air cathode for microbial fuel cell. J. Power Sources 303, 325–332. https://doi.org/10.1016/j.jpowsour.2015.11.003.

Guo, K., Freguia, S., Dennis, P.G., Chen, X., Donose, B.C., Keller, J., Gooding, J.J., Rabaey, K., 2013. Effects of surface charge and hydrophobicity on anodic biofilm formation, community composition, and current generation in bioelectrochemical systems. Environ. Sci. Technol. 47 (13), 7563–7570. https://doi.org/10.1021/es400901u.

Hong, Y., Call, D.F., Werner, C.M., Logan, B.E., 2011. Biosensors and Bioelectronics Adaptation to high current using low external resistances eliminates power overshoot in microbial fuel cells. Biosens. Bioelectron. 28 (1), 71–76. https://doi.org/10.1016/j.bios.2011.06.045.

Lanas, V., Ahn, Y., Logan, B.E., 2014. Effects of carbon brush anode size and loading on microbial fuel cell performance in batch and continuous mode. J. Power Sources 247, 228–234. https://doi.org/10.1016/j.jpowsour.2013.08.110.

Lanas, V., Logan, B.E., 2013. Evaluation of multi-brush anode systems in microbial fuel cells. Bioresour. Technol. 148, 379–385. https://doi.org/10.1016/j.biortech.2013.08.154.

Lawson, K., Rossi, R., Regan, J.M., Logan, B.E., 2020. Impact of cathodic electron acceptor on microbial fuel cell internal resistance. Bioresour. Technol. 316, 123919. https://doi.org/10.1016/j.biortech.2020.123919.

Li, B., Zhou, J., Zhou, X., Wang, X., Li, B., Santoro, C., Grattieri, M., Babanova, S., Artyushkova, K., Atanassov, P., Schuler, A.J., 2014a. Surface modification of microbial fuel cells anodes: Approaches to practical design. Electrochim. Acta 134, 116–126. https://doi.org/10.1016/j.electacta.2014.04.136.

Li, W.-W., Yu, H.-Q., He, Z., 2014b. Towards sustainable wastewater treatment by using microbial fuel cells-centered technologies. Energy Environ. Sci. 7 (3), 911–924. https://doi.org/10.1039/C3EE43106A.

Liang, P., Huang, X., Fan, M.-Z., Cao, X.-X., Wang, C., 2007. Composition and distribution of internal resistance in three types of microbial fuel cells. Appl. Microbiol. Biotechnol. 77 (3), 551–558. https://doi.org/10.1007/s00253-007-1193-4.

Logan, B., Cheng, S., Watson, V., Estadt, G., 2007. Graphite fiber brush anodes for increased power production in air-cathode microbial fuel cells. Environ. Sci. Technol. 41 (9), 3341–3346. https://doi.org/10.1021/es062644y.

Logan, B.E., 2010. Scaling up microbial fuel cells and other bioelectrochemical systems. Appl. Microbiol. Biotechnol. 85 (6), 1665–1671. https://doi.org/10.1007/s00253-009-2378-9.

Logan, B.E., Hamelers, B., Rozendal, R., Schröder, U., Keller, J., Freguia, S., Aelterman, P., Verstraete, W., Rabaey, K., 2006. Microbial fuel cells: Methodology and technology. Environ. Sci. Technol. 40, 5181–5192. https://doi.org/10.1021/es0605016.

Logan, B.E., Wallack, M.J., Kim, K.-Y., He, W., Feng, Y., Saikaly, P.E., 2015. Assessment of microbial fuel cell configurations and power densities. Environ. Sci. Technol. Lett. 2 (8), 206–214. https://doi.org/10.1021/acs.estlett.5b00180.

Logan, B.E., Zikmund, E., Yang, W., Rossi, R., Kim, K.-Y., Saikaly, P.E., Zhang, F., 2018. Impact of ohmic resistance on measured electrode potentials and maximum power production in microbial fuel Cells. Environ. Sci. Technol. 52 (15), 8977–8985. https://doi.org/10.1021/acs.est.8b0205510.1021/acs.est.8b02055.s001.

Nguyen, M.T., Mecheri, B., Iannaci, A., D'Epifanio, A., Licoccia, S., 2016. Iron/polyindole-based electrocatalysts to enhance oxygen reduction in microbial fuel cells. Electrochim. Acta 190, 388–395. https://doi.org/10.1016/j.electacta.2015.12.105.

Rezaei, F., Xing, D., Wagner, R., Regan, J.M., Richard, T.L., Logan, B.E., 2009. Simultaneous cellulose degradation and electricity production by *Enterobacter cloacae* in a microbial fuel cell. Appl. Environ. Microbiol. 75 (11), 3673–3678. https://doi.org/10.1128/AEM.02600-08.

Rismani-Yazdi, H., Carver, S.M., Christy, A.D., Tuovinen, O.H., 2008. Cathodic limitations in microbial fuel cells: An overview. J. Power Sources 180 (2), 683–694. https://doi.org/10.1016/j.jpowsour.2008.02.074.

Ronen, A., Duan, W., Wheeldon, I., Walker, S., Jassby, D., 2015. Microbial attachment inhibition through low-voltage electrochemical reactions on electrically conducting membranes. Environ. Sci. Technol. 49 (21), 12741–12750. https://doi.org/10.1021/acs.est.5b01281.

Rossi, R., Cario, B.P., Santoro, C., Yang, W., Saikaly, P.E., Logan, B.E., 2019a. Evaluation of electrode and solution area-based resistances enables quantitative comparisons of factors impacting microbial fuel cell performance. Environ. Sci. Technol. 53 (7), 3977–3986. https://doi.org/10.1021/acs.est.8b0600410.1021/acs.est.8b06004.s001.

Rossi, R., Evans, P.J., Logan, B.E., 2019b. Impact of fl ow recirculation and anode dimensions on performance of a large scale microbial fuel cell. J. Power Sources 412, 294–300. https://doi.org/10.1016/j.jpowsour.2018.11.054.

Rossi, R., Hall, D.M., Wang, X.u., Regan, J.M., Logan, B.E., 2020. Quantifying the factors limiting performance and rates in microbial fuel cells using the electrode potential slope analysis combined with electrical impedance spectroscopy. Electrochim. Acta 348, 136330. https://doi.org/10.1016/j.electacta.2020.136330.

Rossi, R., Jones, D., Myung, J., Zikmund, E., Yang, W., Gallego, Y.A., Pant, D., Evans, P.J., Page, M.A., Cropek, D.M., Logan, B.E., 2019c. Evaluating a multi-panel air cathode through electrochemical and biotic tests. Water Res. 148, 51–59. https://doi.org/10.1016/j.watres.2018.10.022.

Rossi, R., Logan, B.E., 2020. Unraveling the contributions of internal resistance components in two-chamber microbial fuel cells using the electrode potential slope analysis. Electrochim. Acta 348, 136291. https://doi.org/10.1016/j.electacta.2020.136291.

Rossi, R., Yang, W., Setti, L., Logan, B.E., 2017. Assessment of a metal–organic framework catalyst in air cathode microbial fuel cells over time with different buffers and solutions. Bioresour. Technol. 233, 399–405. https://doi.org/10.1016/j.biortech.2017.02.105.

Saito, T., Mehanna, M., Wang, X., Cusick, R.D., Feng, Y., Hickner, M.A., Logan, B.E., 2011. Effect of nitrogen addition on the performance of microbial fuel cell anodes. Bioresour. Technol. 102 (1), 395–398. https://doi.org/10.1016/j.biortech.2010.05.063.

Saito, T., Merrill, M.D., Watson, V.J., Logan, B.E., Hickner, M.A., 2010. Investigation of ionic polymer cathode binders for microbial fuel cells. Electrochim. Acta 55 (9), 3398–3403. https://doi.org/10.1016/j.electacta.2010.01.009.

Santoro, C., Arbizzani, C., Erable, B., Ieropoulos, I., 2017. Microbial fuel cells: From fundamentals to applications. A review. J. Power Sources 356, 225–244. https://doi.org/10.1016/j.jpowsour.2017.03.109.

Sleutels, T.H.J.A., Lodder, R., Hamelers, H.V.M., Buisman, C.J.N., 2009. Improved performance of porous bio-anodes in microbial electrolysis cells by enhancing mass and charge transport. Int. J. Hydrogen Energy 34 (24), 9655–9661. https://doi.org/10.1016/j.ijhydene.2009.09.089.

Wan, J., Gu, J., Zhao, Q., Liu, Y., 2016. COD capture: A feasible option towards energy self-sufficient domestic wastewater treatment. Sci. Rep. 6, 1–9. https://doi.org/10.1038/srep25054.

Wang, X., Cheng, S., Feng, Y., Merrill, M.D., Saito, T., Logan, B.E., 2009. Use of carbon mesh anodes and the effect of different pretreatment methods on power production in microbial fuel cells. Environ. Sci. Technol. 43 (17), 6870–6874. https://doi.org/10.1021/es900997w.

Wang, X., Li, D., Mao, X., Yu, E.H., Scott, K., Zhang, E., Wang, D., 2016. Anion exchange polymer coated graphite granule electrodes for improving the performance of anodes in unbuffered microbial fuel cells. J. Power Sources 330, 211–218. https://doi.org/10.1016/j.jpowsour.2016.09.019.

Wang, X.u., Xu, C., Golding, B.T., Sadeghi, M., Cao, Y., Scott, K., 2011. A novel phosphoric acid loaded quaternary 1,4-diazabicyclo-[2.2.2]-octane polysulfone membrane for intermediate temperature fuel cells. Int. J. Hydrogen Energy 36 (14), 8550–8556. https://doi.org/10.1016/j.ijhydene.2011.03.143.

Watson, V.J., Logan, B.E., 2011. Analysis of polarization methods for elimination of power overshoot in microbial fuel cells. Electrochem. Commun. 13 (1), 54–56. https://doi.org/10.1016/j.elecom.2010.11.011.

Wen, Q., Wu, Y., Cao, D., Zhao, L., Sun, Q., 2009. Electricity generation and modeling of microbial fuel cell from continuous beer brewery wastewater. Bioresour. Technol. 100 (18), 4171–4175. https://doi.org/10.1016/j.biortech.2009.02.058.

Yang, W., Kim, K.-Y., Saikaly, P.E., Logan, B.E., 2017. The impact of new cathode materials relative to baseline performance of microbial fuel cells all with the same architecture and solution chemistry. Energy Environ. Sci. 10 (5), 1025–1033. https://doi.org/10.1039/C7EE00910K.

Yang, W., Logan, B.E., 2016. Immobilization of a metal-nitrogen-carbon catalyst on activated carbon with enhanced cathode performance in microbial fuel cells. ChemSusChem 9 (16), 2226–2232. https://doi.org/10.1002/cssc.201600573.

Yang, Z.-C., Cheng, Y.-Y., Zhang, F., Li, B.-B., Mu, Y., Li, W.-W., Yu, H.-Q., 2016. Rapid detection and enumeration of exoelectrogenic bacteria in lake sediments and a wastewater treatment plant using a coupled WO_3 nanoclusters and most probable number method. Environ. Sci. Technol. Lett. 3 (4), 133–137. https://doi.org/10.1021/acs.estlett.6b0011210.1021/acs.estlett.6b00112.s001.

Zhang, F., Yuan, S.J., Li, W.W., Chen, J.J., Ko, C.C., Yu, H.Q., 2015. WO3 nanorods-modified carbon electrode for sustained electron uptake from *Shewanella oneidensis* MR-1 with suppressed biofilm formation. Electrochim. Acta 152, 1–5. https://doi.org/10.1016/j.electacta.2014.11.103.

Zhang, X., Pant, D., Zhang, F., Liu, J., He, W., Logan, B.E., 2014. Long-term performance of chemically and physically modified activated carbons in air cathodes of microbial fuel cells. ChemElectroChem 1 (11), 1859–1866. https://doi.org/10.1002/celc.v1.1110.1002/celc.201402123.

Zhang, X., Wang, Q., Xia, X., He, W., Huang, X., Logan, B.E., 2017. Addition of conductive particles to improve the performance of activated carbon air-cathodes in microbial fuel cells. Environ. Sci. Water Res. Technol. 3 (5), 806–810. https://doi.org/10.1039/C7EW00108H.

Zhou, S., Tang, J., Yuan, Y., Yang, G., Xing, B., 2018. TiO_2 nanoparticle-induced nanowire formation facilitates extracellular electron transfer. ACS Energy Lett 5 (9), 564–570. https://doi.org/10.1021/acs.estlett.8b0027510.1021/acs.estlett.8b00275.s001.

Zhu, X., Tokash, J.C., Hong, Y., Logan, B.E., 2013. Controlling the occurrence of power overshoot by adapting microbial fuel cells to high anode potentials. Bioelectrochem. 90, 30–35. https://doi.org/10.1016/j.bioelechem.2012.10.004.